Catalysis Letters Vol. 102, Nos. 3–4, August 2005 (© 2005)
DOI: 10.1007/s10562-005-5864-4

Nanometric $La_{1-x}K_x$ MnO_3 Perovskite-type oxides – highly active catalysts for the combustion of diesel soot particle under loose contact conditions

Hong Wang[a,b], Zhen Zhao[a,*], Chun-ming Xu[a], and Jian Liu[a]

[a]*State Key Laboratory of Heavy Oil Processing, University of Petroleum, Beijing, 102249 China*
[b]*Beijing Institute of Petrochemical Technology, Beijing, 102617 China*

Received 16 March 2005; accepted 19 April 2005

The $La_{1-x}K_xMnO_3$ perovskite-type oxides whose sizes were in nanometric range were prepared by the citric acid-ligated method. The structures of these perovskite-type oxides were examined by XRD and FT-IR. The catalytic activity for the combustion of soot particulate was evaluated by a technique of the temperature-programmed reaction. In the $LaMnO_3$ catalyst, the partial substitution of K for La at A-site enhanced the catalytic activity for the combustion of soot particle. In the $La_{1-x}K_xMnO_3$ catalysts, the combustion temperature of soot particle decreases with increasing x values. The $La_{1-x}K_xMnO_3$ oxides with the substitution quantity between $x=0.20$ and $x=0.25$ are good candidate catalysts for the soot particle removal reaction, and the combustion temperature of soot particle is between 285 and 430 °C when the contact of catalysts and soot is loose, and their catalytic activities for the combustion of soot particle are as good as supported Pt catalysts, which is the best catalyst system so far reported for soot combustion under loose contact conditions.

KEY WORDS: perovskite-type oxides; soot; diesel exhaust; combustion.

1. Introduction

Soot particulate (PM) emitted from diesel engines is a serious contamination in urban area. The carbon is the basic component of soot. The soot drew into the lungs by breathing does much harm to the health because of some organic compounds, heavy metals and many carcinogens adsorbed on the surface of soot. The strict emission control regulations were constituted in USA, Japan and many Europe countries. EURO IV, to be enforced in 2005, will impose to never exceed 0.025 g/km on an ECE-EUDC standard driving cycle [1].

The most promising technology in the field of soot removal is based on wall-flow type catalytic traps, periodically regenerated by the combustion of soot. The temperature of diesel exhaust gases, generally between 150 and 450°C, is lower, however, the combustion of the trapped soot is above 550°C [2]. The role of the catalyst here is to reduce soot ignition temperature and enhance the combustion rate of the soot collected on the filter during trap regeneration [3]. Under practical conditions, the contact between the catalysts on the surface of filter and PM particle is loose [4,5]. Therefore, it is rather significant to study and design the active catalysts for soot particulate oxidation under loose contact conditions. Methods for the increasing catalyst-soot contact include metal fuel additives and using mobile catalytic compounds. Using metal additives may increase ash formation and cause clogging of the filter. High catalyst mobility can be achieved by using low melting point eutectic mixtures of oxides or Chloride-containing mixtures. In this respect, Cu/K/V/Cl or Cu/K/Mo/Cl have lower melting points than the mixtures of only metal oxides and are highly active for oxidation of soot by O_2 [4–7]. However, Chloride-containing catalysts are considered to be impractical because of their high volatility and potential toxicity. In recent years, Oi-Uchisawa *et al.* reported that SO_2 and H_2O present in the reactant in addition to NO substantially promote soot oxidation over Pt catalysts [8–10]. In the catalyst system, platinum is supposed to promote soot oxidation indirectly, i.e., by oxidizing the NO to NO_2, which subsequently oxdizes soot to CO and CO_2. The one is the best catalyst system so far reported for soot combustion under loose contact conditions.

Several authors [11–14] have reported that perovskite-type oxides are active for simultaneous NO_x-soot removal reaction. In addition, the substitutional incorporation of K into A-sites of perovskite-type (ABO_3) oxides was found to be quite effective in enhancing the activity and selectivity for the NO_x–O_2–soot reaction [13–16]. Teraoka *et al.* found that La–K–Mn–O perovskite-type oxides are good candidate catalysts for diesel soot combustion under tight conditions [17], but they did not report the relevant catalytic activities under loose contact conditions.

* To whom correspondence should be addressed.
E-mail: zhenzhao@bjpeu.edu.cn

In this work, the nanometric $La_{1-x}K_xMnO_3$ perovskite-type oxides were prepared by the citric acid-ligated method, and it was investigated that the substitution contents of A-site cation affect on the structure and catalytic performances for soot particle combustion under loose contact conditions. It has been found that the nanometric $La_{1-x}K_xMnO_3$ oxides with the substitution quantity between $x=0.20$ and $x=0.25$ are good candidate catalysts for the soot particle removal reaction under loose contact conditions. The probable reasons that can lead to the activity enhancement for the K substitution samples compared to the unsubstitution sample ($LaMnO_3$) were discussed.

2. Experimental

2.1. Catalyst preparation

A series of $La_{1-x}K_xMnO_3$ ($x=0$–0.35) perovskite-type oxide samples were prepared by the citric acid-ligated method. The nitrates of La, K and Mn^{2+} were used as starting materials for obtaining an aqueous solution of La^{3+}, K^+ and Mn^{2+} with appropriate stoichiometry. A solution of citric acid 100% in excess was added. The resulting solution was heated and evaporated to dryness with vigorous stirring, following burning or explosion and finally the precursor was calcined at 800°C for 6 h in static air. This technique is particularly suitable to producing nanosized particle samples.

2.2. Catalyst characterization

The crystal structures of the fresh catalysts were determined by a powder X-ray diffractometer (Shimadzu XRD 6000), using Cu K α ($\lambda = 1.54184$ Å) radiation combined with Niche filter operating at 40 KV and 10 mA. The diffractometer data were recorded for 2θ values between 15 and 70° and scanning rate was 8°/min.

FT-IR spectra were recorded on a Digilab FTS-3000 spectrophotometer. The measured wafer was prepared as KBr pellet with the weight ratio of sample to KBr, 1/100. The resolution was set at 2 cm^{-1} during measurement.

The morphology of the catalysts were observed by SEM (S-5200, Japan).

The BET specific surface area of the studied samples were measured with linear parts of the BET plot of the N_2 isotherms, using a Micromeritics ASAP 2010 analyzer.

2.3. Activity measurement

Printex-U which was supplied by Degussa was used as model soot. Its primary particle size was 25 nm and specific surface was 100 $m^2\ g^{-1}$. The catalytic activity was evaluated by a temperature-programmed oxidation reaction (TPR) apparatus, a quartz microreactor (i.d. = 6 mm) at atmospheric pressure. A standard gas mixture composition was 2000 ppm NO, 5% O_2 with He dilution. A 100 mg soot and catalyst (ratio 1:10, w/w) was loaded in the middle of the reactor tube with quartz wool. The soot and catalyst were mixed with a spatula in order to reproduce the loose contact mode, which is the most representative model of diesel particles flowing through a catalytic filter. The outlet gas composition was analyzed by gas chromatography (Sp-3420, Beijing) with TCD using columns of Proapak Q (for the separation of CO_2, N_2O) and molecular sieve 5A (for the separation of O_2, N_2, CO, NO).

From TPR results, three parameters were derived in order to evaluate the catalytic performances of the catalysts for soot combustion. The first one was the ignition temperature of soot (T_{ig}) estimated by extrapolating the steeply ascending portion of the carbon dioxide formation curve to zero carbon dioxide concentration, and the second one was the temperature corresponding to the soot maximal combustion rate (T_m) and the last one was the final combustion temperature (T_f) obtained by extrapolating the steeply descending portion of the carbon dioxide formation curve to zero carbon dioxide concentration. The CO_2 outlet concentration increases starting from the carbon ignition temperature, reaches a maximum, and then decreases as a consequence of carbon consumption. The temperature corresponding to the CO_2 peak (T_m) can be taken as an index of the activity of each tested catalyst. The lower the T_m value, the more active the catalyst.

3. Results and discussion

3.1. Catalyst characterization

The XRD patterns of the $La_{1-x}K_xMnO_3$ oxides are shown in figure 1. The XRD patterns of all the samples give a large peak at 33°, and the d values of characteristic pedigrees are 2.74, 1.94 and 1.59, which is consistent with the references [17–19]. These results indicate that the complex oxides of $La_{1-x}K_xMnO_3$ possessed ABO_3 perovskite-type structures. For $La_{0.70}K_{0.30}MnO_3$ and $La_{0.65}K_{0.35}MnO_3$ catalysts, additional peak not belonging to the perovskite phase was observed at 25.2^o and they could be assigned to $K_2Mn_4O_8$, and the formation of $K_2Mn_4O_8$ in a trace amount was also confirmed in the $La_{0.75}K_{0.25}MnO_3$ catalyst [17].

Table 1 shows the crystal particle sizes of $La_{1-x}K_xMnO_3$ samples. The average crystal particle sizes of $La_{1-x}K_xMnO_3$ samples were in the range of 14–33 nm. The results reveal that $La_{1-x}K_xMnO_3$ samples which were prepared by the citric acid-ligated method possessed nanometric particles.

Figure 2 shows IR spectra of $La_{1-x}K_xMnO_3$ perovskite-oxides. In the whole range of $0.35 \geq x \geq 0$, this series of samples all have the vibration bands around

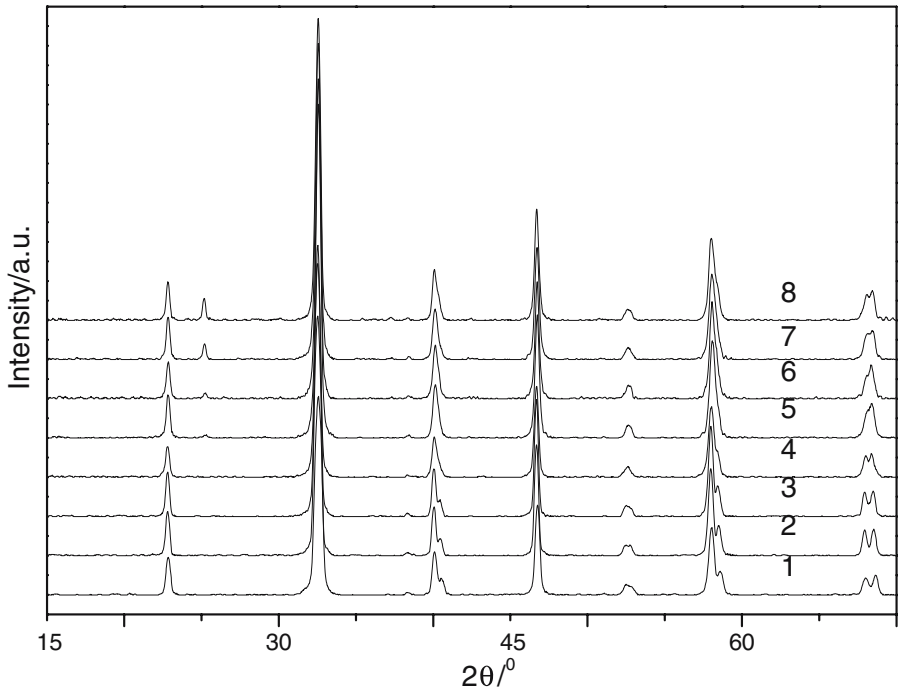

Figure 1. X-ray diffraction patterns of $La_{1-x}K_xMnO_3$ catalysts (1). $LaMnO_3$ (2). $La_{0.95}K_{0.05}MnO_3$ (3). $La_{0.90}K_{0.10}MnO_3$ (4). $La_{0.85}K_{0.15}MnO_3$ (5). $La_{0.80}K_{0.20}MnO_3$ (6). $La_{0.75}K_{0.25}MnO_3$ (7). $La_{0.70}K_{0.30}MnO_3$ (8). $La_{0.65}K_{0.35}MnO_3$.

Table 1
The average crystal size of $La_{1-x}K_xMnO_3$ catalysts

$x=0$		$x=0.05$		$x=0.10$		$x=0.15$		$x=0.20$		$x=0.25$		$x=0.30$		$x=0.35$	
$2\theta/^0$	D/nm	$2\theta/^0$	D/nm	$2\theta/^0$	D/nm	$2\theta/^0$	D/nm	$2\theta/^0$	D/nm	$2\theta/^0$	D/nm	$2\theta/^0$	D/nm	$2\theta/^0$	D/nm
32.57	14.75	32.58	16.15	32.50	17.63	32.65	20.41	32.54	21.10	32.65	25.12	32.67	22.32	32.63	22.12
46.77	24.47	46.75	24.34	46.67	26.85	46.84	29.75	46.71	27.02	46.84	24.48	46.88	32.96	46.81	25.57
58.04	19.98	58.01	23.41	57.96	22.85	58.18	20.92	58.07	21.01	58.20	19.78	58.20	19.70	58.14	19.56

600 cm^{-1}, which have been attributed to the characteristic vibration band of perovskite-type (ABO_3) oxides [20]. This result shows that the series of $La_{1-x}K_xMnO_3$ all have the structure of ABO_3 type. MnO_6 octahedron, which have A-site cation in their clearance, is the unit cell of $La_{1-x}K_xMnO_3$ crystalline structure. There are six vibrancies to IR spectra [20], and the stretching vibration (v_3) is inactive if three pairs of Mn–O bonds have the same lengths, i.e., MnO_6 octahedron having higher symmetry. On the contrary, the Mn–O stretching vibration v_3 is active if the symmetry of MnO_6 is low. It is obvious that the intensity of the vibration band at around 600 cm^{-1} decrease with x increasing in $La_{1-x}K_xMnO_3$ oxides, especially when $x \geq 0.15$, the vibration band become much weak, broad and upshifting. These results indicate that some amounts of Mn^{3+} changed into Mn^{4+} when some La^{3+} was replaced by K^+. Two new vibration bands at around 480, 520 cm^{-1} appeared when K^+ substitution amount is equal to or exceeds 0.25. In order to assign these bands, the FT-IR spectra of K_2O and K_2CO_3 were recorded and their vibration bands were not located around 500 cm^{-1}, which was not showed here for simplicity. These new two bands maybe due to the formation of K–Mn compound other than La–Mn–O perovskite oxide when K substitution amount is greater than 0.25 [17].

SEM photographs of $LaMnO_3$ and $La_{0.75}K_{0.25}MnO_3$ perovskite-oxides are presented in figure 3. The SEM image of $La_{0.75}K_{0.25}MnO_3$ shows that the catalyst particles had an average particle size centered around 50 nm with a spherical shape, and it has a much better dispersion than unsubstituted sample $LaMnO_3$.

The specific surface area of the perovskite-oxides is shown in the Table 2. The BET surface area of $La_{1-x}K_xMnO_3$ catalysts is between 9 m^2/g and 18 m^2/g.

3.2. Catalytic activity for soot combustion

The TPR curves as shown in figure 4 are useful to compare the catalytic activity of the catalysts for soot combustion. Compared with blank case (i.e., without catalyst) the temperature for soot combustion was lowered down by 180°C for $LaMnO_3$ as catalyst (seen

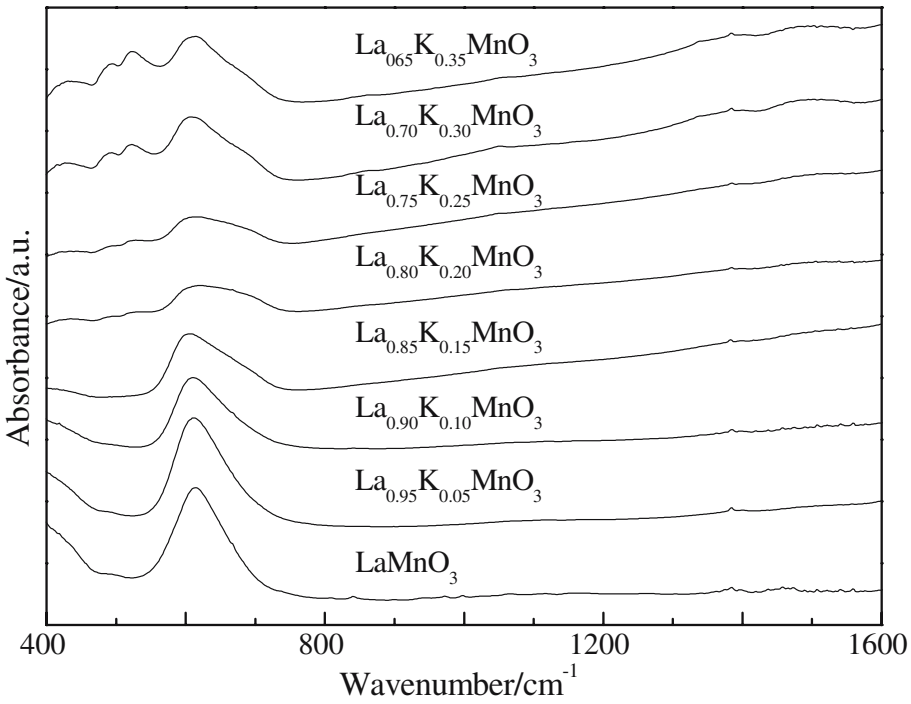

Figure 2. FT-IR spectra of $La_{1-x}K_xMnO_3$ catalysts.

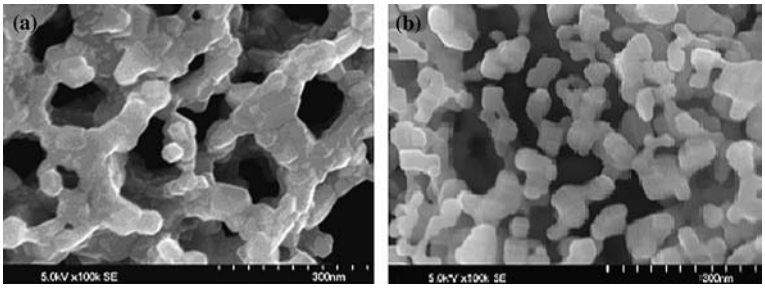

Figure 3. SEM photographs obtained for catalysts after calcination at 800°C (a) $LaMnO_3$ (b) $La_{0.75}K_{0.25}MnO_3$.

Table 2
Specific surface area of $La_{1-x}K_xMnO_3$ catalysts

Catalysts	Specific surface area/m^2/g	Catalysts	Specific surface area/m^2/g
$LaMnO_3$	12.7	$La_{0.80}K_{0.20}MnO_3$	18.2
$La_{0.95}K_{0.05}MnO_3$	11.9	$La_{0.75}K_{0.25}MnO_3$	16.7
$La_{0.90}K_{0.10}MnO_3$	11.7	$La_{0.70}K_{0.30}MnO_3$	13.1
$La_{0.85}K_{0.15}MnO_3$	11.3	$La_{0.65}K_{0.35}MnO_3$	9.5

from figure 4 a). The soot combustion temperatures significantly reduced over all the samples with K substitution for La compared to the unsubstituted sample $LaMnO_3$. (as shown in figure 4 b).

A very interesting phenomenon was found that the catalytic performances of the K-substituted samples can be classified into two groups. One group is for the samples with K-substituted amount $x \leq 0.15$, the other is for the samples with K-substituted amounts $0.15 \leq x \leq 0.35$. The detailed activity data (T_{ig}, T_m, T_f) of the series of $La_{1-x}K_xMnO_3$ oxide catalysts for soot combustion are listed in Table 3. The catalytic activity of $La_{1-x}K_xMnO_3$ oxide catalysts for soot combustion is as good as supported Pt catalyst which is the most active catalyst system so far reported when the contact between soot particle and catalyst surface was loose [21].

3.3. *Relation between the physico-chemical properties of $La_{1-x}K_xMnO_3$ perovskite-type oxides and their catalytic performances.*

It is a complicated multi-phase reaction process for catalytic combustion reaction of soot over catalysts. The nature of soot particle oxidation over catalyst surface should follow redox mechanism containing the reduction and oxidation of the ions in catalyst. There are several main controlling factors which govern the catalytic properties of soot oxidation over the mixed oxide

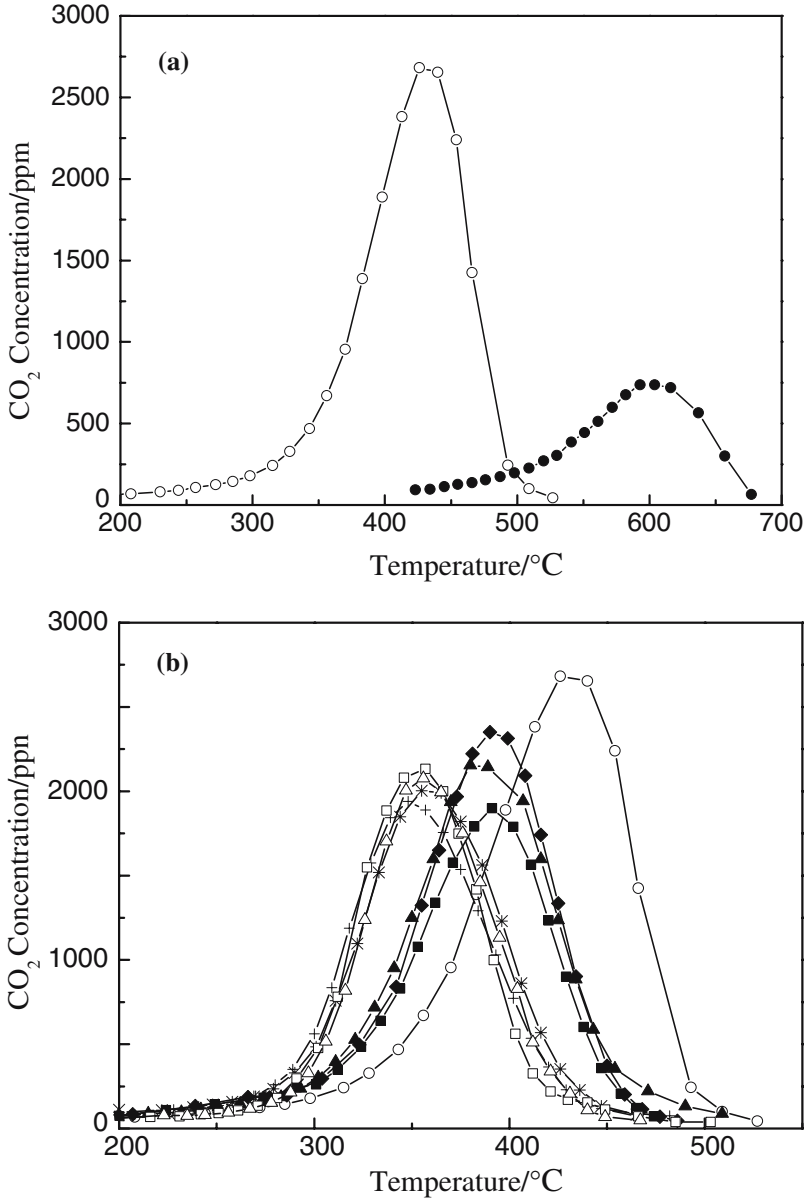

Figure 4. TPR profiles of carbon oxidation over catalysts under loose contact conditions. Reactant gas: 2000 ppm NO + 5% O_2 (a) non-catalyst (■) $LaMnO_3$(—); (b) $LaMnO_3$(—), $La_{095}K_{0.05}MnO_3$(■), $La_{0.90}K_{0.10}MnO_3$(◆), $La_{0.85}K_{0.15}MnO_3$(▲), $La_{0.80}K_{0.20}MnO_3$(), $La_{075}K_{0.25}MnO_3$(+), $La_{0.70}K_{0.30}MnO_3$(□), $La_{0.65}K_{0.35}MnO_3$(△).

catalysts. The first one is the good redox properties of the oxide catalysts, especially the oxidizing ability of B site cation in perovskite-type oxides. This is the most important one for the activation and oxidizing of the soot particle, which is intrinsic properties of the catalyst. The second one is the oxidizing ability of oxidant. For example, NO_2 is stronger oxidant than molecular oxygen. The third one is the good contact between soot particle and catalyst surface, which is indispensable conditions for an active catalyst to play the role on soot combustion.

For perovskite-type oxide catalyst, B-site cations for soot combustion possess the function of catalysis. The cation at A-site (La^{3+}) is generally trivalent, as La^{3+} at A-site is replaced by lower valency cation K^+, according to the principle of electron neutrality, the positive charge reduced could be balanced either by the formation of higher oxidation state ion at B-site [22–27], i.e.,

$$Mn^{3+} \rightarrow Mn^{4+}$$

$$La_{1-x}K_xMn^{3+}_{1-2x}Mn^{4+}_{2x}O_3 \rightarrow LaMnO_{3.} + xLa^{3+}|K^+|'' + 2xMn^{3+}|Mn^{4+}|^{\cdot}$$

or by the formation of oxygen vacancy (V_0) in $La_{1-x}K_xMn\ O_3$.

$$La_{1-x}K_x\lambda(V_0)Mn^{3+}O_{3-\lambda} \rightarrow LaMnO_{3.} + xLa^{3+}|K^+|'' + \lambda|O|^{\cdot\cdot}$$

Table 3
Combustion temperature of carbon particle on $La_{1-x}K_xMnO_3$ catalysts

Serial number	Catalysts	T_{ig}/°C	T_m/°C	T_f/°C
1	$LaMnO_3$	336.6	432.0	497.1
2	$La_{0.95}K_{0.05}MnO_3$	304.7	390.0	456.6
3	$La_{0.90}K_{0.10}MnO_3$	309.6	390.0	457.6
4	$La_{0.85}K_{0.15}MnO_3$	309.6	382.0	457.9
5	$La_{0.80}K_{0.20}MnO_3$	286.9	358.0	432.6
6	$La_{0.75}K_{0.25}MnO_3$	284.6	348.0	429.9
7	$La_{0.70}K_{0.30}MnO_3$	291.5	355.0	419.0
8	$La_{0.65}K_{0.35}MnO_3$	293.7	356.0	429.3

Based on the above discussion, the following three reasons can lead to the activity enhancement for K-substituted samples ($La_{1-x}K_xMnO_3$) compared to the unsubstituted sample ($LaMnO_3$). The first one is that A-site cation (La^{3+}) were replaced partly by K^+ and partial Mn^{3+} changed to Mn^{4+}, which had better catalytic oxidation activity than Mn^{3+}. The second one is the increase in the content of oxygen vacancy (V_0) in $La_{1-x}K_xMn\ O_3$, which increases the adsorption and activation oxygen at catalyst surface. Therefore, it can improve oxidant activity. The last one is that the nanoparticle $La_{1-x}K_xMnO_3$ perovskite-type oxides were obtained. The surface particle sizes of nanoparticle catalyst are small. Surface atoms on surface of nanoparticle catalysts have extra and high surface energies and they are good at mobility. Thus, the contact is still very good between catalysts and soot even under loose contact conditions [4,28].

4. Conclusions

The nanoparticle $La_{1-x}K_xMnO_3$ perovskite-type oxides were obtained by the organic acid- ligated method. In the $LaMnO_3$ catalyst, the partial substitution of K^+ into A-site La^{3+} enhanced the catalytic activity, i.e., the combustion temperature of soot particle decreases with increasing x values. The combustion temperature for soot particle over the samples with K-substitution amount between 0.20 and 0.25 is between 285 and 430°C under loose contact conditions. These catalytic activity for the combustion of soot particle are as good as supported Pt catalysts which is the best catalyst system so far reported for soot combustion under loose contact conditions.

Acknowledgements

This work was supported by the National Natural Science Foundation of China (No. 20473053), the Scientific Research Key Foundation for the Returned Overseas Chinese Scholars of State Education Ministry, and the National Basic Research Program of China (grant No. 2004CB217806).

References

[1] B. Dernaika and D. Uner, Appl. Catal. B 40 (2003) 219.
[2] P. Li, B. Zhu and R. Wang, Chinese Natural Gas Chim. Eng. 20 (1995) 18.
[3] B.A.A.L. van Setten, M. Makkee and J.A. Moulijn, Catal. Rev. Sci. Eng. 43 (2001) 489.
[4] J.P.A. Neeft, M. Michiel and A. Jacob, Appl. Catal. B 8 (1996) 57.
[5] Z. Zhao, A. Obuchi, J. Oi-Uchisawa, A. Ogata and S. Kushiyama, Chem. Lett. 4 (1998) 367.
[6] C. Badini, G. saracco, V. Serra and V. Specchia, Appl. Catal. B 18 (1998) 137.
[7] J.P.A. Neeft, W. Schipper, G. Mul, M. Makkee and J.A. Moulijn, Appl. Catal. B 11 (1997) 365.
[8] J. Oi-Uchishawa, S.D. Wang, T. Nanba, A. Ohi and A. Obuchi, Appl. Catal. B 44 (2003) 207.
[9] J. Oi-Uchishawa, A. Obuchi, R. Enomoto, J.Y. Xu, T. Nanba, S.T. Liu and S. Kushiyama, Appl. Catal. B 32 (2001) 257.
[10] J. Oi-Uchishawa, A. Obuchi, Ryuji, S.D. Wang, T. Nanba and A. Ohi, Appl. Catal. B 43 (2003) 117.
[11] Y. Teraoka, K. Nakano, S. Kagawa and W.F. Shangguan, Appl. Catal. B 5 (1995) L181.
[12] Y. Teraoka, K. Nakano, W.F. Shangguan and S. Kagawa, Catal. Today 27 (1996) 107.
[13] W.F. Shangguan, Y. Teraoka and S. Kagawa, Appl. Catal. B 16 (1998) 149.
[14] S.-S. Hong and G.-D. Lee, Catal. Today 63 (2000) 397.
[15] D. Fino, P. Fino, G. Saracco and V. Specchia, Appl. Catal. B 43 (2003) 243.
[16] T. Miyazaki, N. Tokabuchi, M. Arita, M. Inoue and I. Mochida, Energy & Fuel 11 (1997) 832.
[17] Y. Teraoka, K. Kanada and S. Kagawa, Appl. Catal. B 34 (2001) 73.
[18] D. Weng, H.M. Ding, L.H. Xu, Z. Chen and X.D. Wu, J. Chinese Rare Earth Society 4 (2001) 338.
[19] M. Chen, Y.W. Wang and X.M. Zheng, Chinese J. Inorganic Chem. 10 (2003) 1145.
[20] K.B. LiK, X.J. Li and K.G. Zhu, J. Appl. Phys. 10 (1997) 6943.
[21] J. Oi-Uchishawa, A. Obuchi, Z. Zhao and S. Kushiyama, Appl. Catal. B 18 (1998) L183.
[22] Z. Zhao, X.G. Yang and Y. Wu, Chinese Sci. Bulletin 21 (1995) 1961.
[23] Y. Wu, T. Wu, B.S. Dou, C.X. Wang, X.F. Xie, Z.L. Yu, S.R. Fan, Z.R. Fan and L.C. Wang, J. Catal. 120 (1989) 88.
[24] Y. Wu, Z. Zhao, Y. Liu and X.G. Yang, J. Molecular Catal. A 155 (2000) 89.
[25] Z. Zhao, X. Yang and Y. Wu, Appl. Catal. B 8 (1996) 281.
[26] H. Falcon, M.J. Martinez-Lope, J.A. Alonso and J.L.G. Fierro, Appl. Catal. B 26 (2003) 131.
[27] F. Debora, F. Paolo, S. Guido and S. Vito, Appl. Catal. B 43 (2003) 243.
[28] B.R. Stanmore, J.F. Brilhac and P. Gilot, Carbon 39 (2001) 2247.